Super-resolution imaging in optical scanning holography using structured illumination

Zhenbo Ren, Edmund Y. Lam

Zhenbo Ren, Edmund Y. Lam, "Super-resolution imaging in optical scanning holography using structured illumination," Proc. SPIE 10022, Holography, Diffractive Optics, and Applications VII, 1002203 (31 October 2016); doi: 10.1117/12.2247791

SPIE.

Event: SPIE/COS Photonics Asia, 2016, Beijing, China

Invited Paper

Super-Resolution Imaging in Optical Scanning Holography using Structured Illumination

Zhenbo Ren and Edmund Y. Lam

Department of Electrical and Electronic Engineering, The University of Hong Kong, Pokfulam, Hong Kong, China

ABSTRACT

As a specific digital holographic microscopy system, optical scanning holography (OSH) is an appealing technique that makes use of the advantages of holography in the application of optical microscopy. In OSH system, a three-dimensional object is scanned with a Fresnel zone plate in a raster fashion, and the electrical signals are demodulated into a complex hologram by heterodyne detection. Then the recorded light wavefront information contained in the hologram allows one to digitally reconstruct the specimen for multiple purposes such as optical sectioning, extended focused imaging as well as three-dimensional imaging. According to Abbe criterion, however, akin to those conventional microscopic imaging systems, OSH suffers from limited resolving power due to the finite sizes of the objective lens and the aperture, i.e., low numerical aperture. To bypass the diffraction barrier in light microscopy, various super-resolution imaging techniques have been proposed. Among those methods, structured illumination is an ensemble imaging concept that modulates the spatial frequency by projecting additional well-defined patterns with different orientation and phase shift onto the specimen. Computational algorithms are then applied to remove the effect of the structure and to reconstruct a super-resolved image beyond the diffraction-limit. In this paper, we introduce this technique in OSH system to scale down the spatial resolution beyond the diffraction limit. The performance of the proposed method is validated by simulation and experimental results.

Keywords: super-resolution imaging, OSH, structured illumination

1. INTRODUCTION

Digital holographic microscopy (DHM) is an important and attractive application of holography in light microscopy due to its capabilities to numerically focus on different planes without mechanical movement, to correct optical aberrations, and to compute the intensity and phase distributions simultaneously.[1] Unlike traditional wide-field microscopy which only records a projected intensity image of a three-dimensional (3D) object, DHM can digitally record the wavefront information emanated from the specimen as a 2D hologram with a photodetector. Numerical post-processing, which simulates the back propagation of the wavefront, allows one to obtain an intensity or phase image, 3D image or achieve refocusing on different depths etc, with respective reconstruction algorithms. This flexibility enables DHM to be used in a wide range such as pattern recognition in integrated circuit and particle tracking in fluid mechanics.[2]

However, DHM suffers the same problem of limited resolving power as conventional microscopy. The photodetector and the numerical aperture (NA) of the objective lens drastically limit the resolution of a light microscope. In the viewpoint of Fourier optics, a microscope can be regarded as a low-pass filter. An objective lens with finite size has a finite support from the optical transfer function (OTF) in frequency domain. Only low frequency components of the spectrum emitted by the object can pass through and be recorded by the photodetector.[3] As a consequence, owing to the absence of high spatial frequency components, the recorded image loses fine details and becomes blurred. Diffraction limit is used to estimate the limiting resolving power of a microscope that can discern two closely positioned elements of a structure.[4] According to Abbe criterion, the minimal distance $(\delta x_{min}, \delta y_{min})$ that can be resolved in the lateral plane is approximated by $0.61\lambda/\text{NA}$, where λ is the working

Further author information: (Send correspondence to E. Y. L.)
E. Y. L.: E-mail: elam@eee.hku.hk

Holography, Diffractive Optics, and Applications VII, edited by Yunlong Sheng, Chongxiu Yu, Changhe Zhou, Proc. of SPIE Vol. 10022, 1002203 · © 2016 SPIE
CCC code: 0277-786X/16/$18 · doi: 10.1117/12.2247791

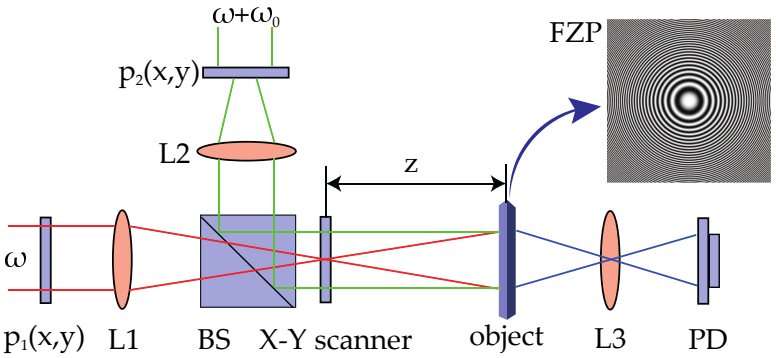

Figure 1: Schematic diagram of OSH system. ω and ω_0 are initial carrier frequency of the laser source and the shifted frequency; $p_1(x, y)$ and $p_2(x, y)$ are pupils; L1, L2 and L3 are lenses; BS is beam splitter; X-Y scanner is 2D scanning mirror; Object is the specimen to be recorded; PD is photodetector; z is the distance between the object and the scanner.

wavelength, $\mathrm{NA} = n \cdot \sin(\theta)$ of the objective lens, n is the refractive index of the immersion medium, θ is half the aperture angle of the objective lens. The resolution in the longitudinal direction is normally worse, and can be approximated by the expression $\delta z_{min} = 2\lambda/\mathrm{NA}^2$. Emitters that have a distance smaller than this magnitude are impossible to be distinguished.[5–7]

This paper proposes to incorporate structured illumination in a specific DHM system, optical scanning holography (OSH), to improve the spatial resolution beyond the diffraction limit. The principle and optical setup of this combination are described in details below. Simulated and experimental data verify the feasibility of the proposed approach.

2. PRINCIPLE OF OSH

Fig. 1 presents a conventional OSH imaging system. On the object plane, two beams with a slight difference in frequency interfere and generate a time-dependent interference pattern, which scans the 3D specimen actively. The intensity of the transmitted light is collected by a photodetector. Other than direct detection, in OSH heterodyne detection is used to demodulate the intensity signal into real and imaginary parts composing a complex hologram. Thus a 2D digital hologram containing the entire 3D information of the object is obtained.[8,9] The schematic diagram of the OSH imaging system is shown in Fig. 1.

Mathematically, the OTF of the OSH system is[10]

$$\mathcal{H}(k_x, k_y; z) = \exp\left[j\frac{z}{2k_0}(k_x^2 + k_y^2)\right] \cdot \int_{-\infty}^{+\infty}\int_{-\infty}^{+\infty} p_1^{\dagger}(x, y) p_2\left(x + \frac{f}{k_0}k_x, y + \frac{f}{k_0}k_y\right) \exp\left[j\frac{z}{f}(xk_x + yk_y)\right] dxdy, \quad (1)$$

where $\dagger$ denotes complex conjugate, (x, y) are spatial coordinates, (k_x, k_y) are frequency coordinates, $k_0 = 2\pi/\lambda$ is wavenumber, f is the focal distance of L1 and L2, z is propagation distance. Then the point spread function (PSF) of the system can be obtained as $h(x, y; z) = \mathfrak{F}^{-1}\left\{\mathcal{H}(k_x, k_y; z)\right\}$ using the inverse Fourier transform.[11]

The scanning pattern is the interference of the two beams passing through $p_1(x, y)$ and $p_2(x, y)$. For mathematical simplicity, two pupils are usually chosen as $p_1(x, y) = 1$ and $p_2(x, y) = \delta(x, y)$, producing a plane wave and a diverging spherical wave.[12] Therefore the illumination pattern is a Fresnel zone plate (FZP), which is shown in Fig. 1. By selecting proper pupils, one can acquire different illumination patterns, as well as different PSFs to improve the performance of the system.[13]

The OSH system is linear and time-invariant. Suppose the object to be recorded is discrete with multiple sections. The hologram $g(x, y)$ is given by $g(x, y) = o(x, y; z) * h(x, y; z)$, where $*$ denotes 2D convolution, z is the distance of each section. In the Fourier domain, it becomes

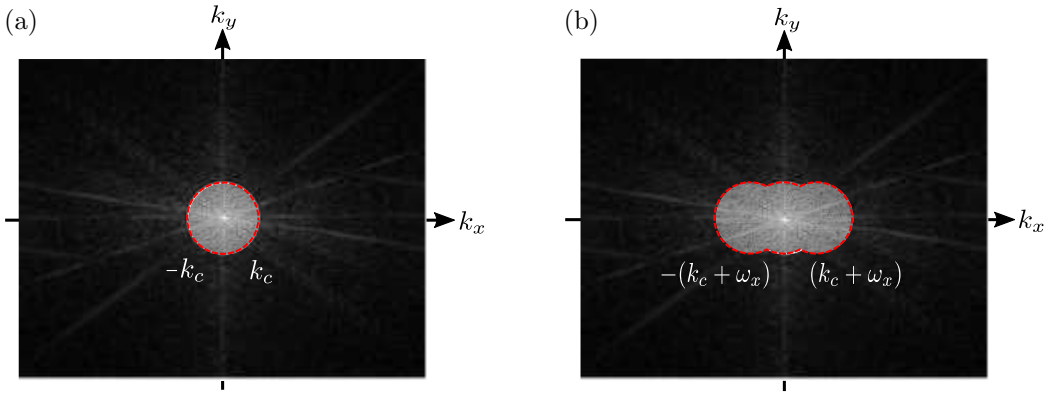

Figure 2: (a) Conventional OSH acts as a low-pass filter that only allows the spectrum in the passband to go through. (b) SI-OSH duplicates the object's spectrum in two horizontal directions and thus enlarges the obtained frequency components.

$$\mathcal{G}(k_x, k_y) = \mathcal{O}(k_x, k_y; z) \cdot \mathcal{H}(k_x, k_y; z). \tag{2}$$

In numerical reconstruction, the conventional approach, which convolves the hologram with the complex conjugation of PSF, possibly leads to a corrupted image due to the defocus noise when the recorded object consists of multiple sections. Here we employ the inverse imaging technique, making use of the block Jacobi-type restrictive preconditioned conjugate gradient (BJ-RPCG) algorithm, so as to suppress noise and reconstruct sectional images.[14]

3. STRUCTURED ILLUMINATION OSH

The basic principle of structured illumination is to employ the moiré effect generated by frequency mixing. The coarse pattern multiplicatively superimposed by two fine signals enables one to gain access to the high frequency components that are normally undetectable by the imaging system under careful control and reconstruction.[15,16] In structured illumination, when the sample is under sinusoidal patterned illumination, high frequency components beyond the cutoff frequency are moved into the bandwidth of the OTF, thus becoming observable by the optical imaging system. After extracting the shifted high frequency components using phase shifting patterns, a super-resolved image is then reconstructed.[17] Fig. 2 illustrates the principle of bypassing the diffraction limit by using structured illumination.[18]

As mentioned above, in OSH system an interference pattern FZP scans the object in a 2D fashion. Compared with the uniform illumination in wide-field microscopy, the FZP that illuminates the sample can be regarded as a structured light. However, this illumination scheme is not able to improve its resolution performance since in frequency domain, the spectrum of the object is not duplicated such that high frequency components that are not observable before are still outside the passband of the OTF. In this section, an optical setup incorporating structured illumination with OSH system (SI-OSH) and the simulation results are presented, and we explain how to overcome the diffraction limit with the proposed system in Fig. 3.

The illumination pattern is conventionally sinusoidal, and projected onto the sample. Sinusoidal pattern can be generated in different ways such as grating or spatial light modulator. Here we adopt the scheme of using a diffraction grating. The transmittance function of a 2D grating can be expressed as[19,20]

$$t(x, y) = I_0 \left[1 + \frac{m}{2}\cos(\omega_x x) + \frac{m}{2}\cos(\omega_y y)\right], \tag{3}$$

where ω_x and ω_y are spatial frequencies in horizontal and vertical directions, I_0 and m are constants denoting the mean intensity and modulation depth, respectively. Suppose the focal distance of L1 is also f. The wavefront at the back focal plane is the Fourier transform of Eq. 3, i.e.,

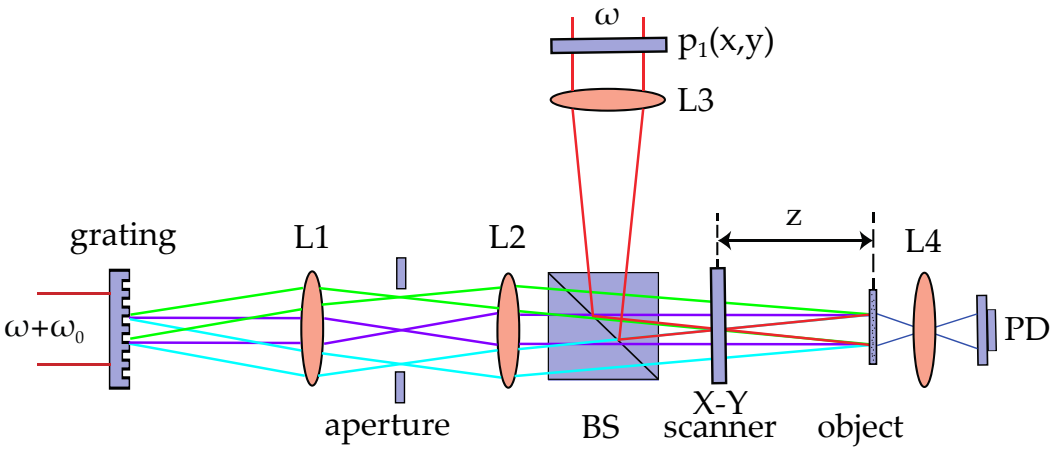

Figure 3: Schematic diagram of SI-OSH system.

$$\begin{aligned} t'(x,y) &= \mathfrak{F}^{-1}\{t(x,y)\}\Big|_{k_x=k_0x/f,\ k_y=k_0y/f} \\ &= I_0\pi\left[\delta\left(\frac{k_0x}{f},\frac{k_0y}{f}\right)+\frac{m}{2}\delta\left(\frac{k_0x}{f}-\omega_x,\frac{k_0y}{f}-\omega_y\right)+\frac{m}{2}\delta\left(\frac{k_0x}{f}+\omega_x,\frac{k_0y}{f}+\omega_y\right)\right] \\ &= t'_1(x,y)+t'_2(x,y)+t'_3(x,y), \end{aligned} \tag{4}$$

where $t'_1(x,y)=\delta(\frac{k_0x}{f},\frac{k_0y}{f})$, $t'_2(x,y)=\delta(\frac{k_0x}{f}-\omega_x,\frac{k_0y}{f}-\omega_y)$, and $t'_3(x,y)=\delta(\frac{k_0x}{f}+\omega_x,\frac{k_0y}{f}+\omega_y)$. We omit the constants here as well as in the following derivations. In the proposed system, this wavefront is then processed in the same way as the wavefront at the pinhole plane, which is denoted as $p_2(x,y)$ in the conventional OSH system. Substitute Eq. 4 into Eq. 1 and select $p_1(x,y)=1$, we then have

$$\begin{aligned} \mathcal{H}'(k_x,k_y;z) &= \mathcal{H}_0\cdot\int_{-\infty}^{+\infty}\int_{-\infty}^{+\infty}t'\left(x+\frac{f}{k_0}k_x,y+\frac{f}{k_0}k_y\right)\exp\left[j\frac{z}{f}(xk_x+yk_y)\right]dxdy \\ &= \mathcal{H}'_1(k_x,k_y;z)+\mathcal{H}'_2(k_x,k_y;z)+\mathcal{H}'_3(k_x,k_y;z), \end{aligned} \tag{5}$$

where $\mathcal{H}_0(k_x,k_y;z)=\exp[j\frac{z}{2k_0}(k_x^2+k_y^2)]$, $\mathcal{H}'_i(k_x,k_y;z)=\mathcal{H}_0\cdot\int_{-\infty}^{+\infty}\int_{-\infty}^{+\infty}t'_i(x+\frac{f}{k_0}k_x,y+\frac{f}{k_0}k_y)\exp[j\frac{z}{f}(xk_x+yk_y)]dxdy$, $i=1,2,3$. As shown in Eq. 4, there are three diffraction orders after the grating, leading to three terms in the new OTF. We then have the analytical expressions of the first term as

$$\begin{aligned} \mathcal{H}'_1(k_x,k_y;z) &= \mathcal{H}_0\cdot\int_{-\infty}^{+\infty}\int_{-\infty}^{+\infty}t'_1\left(x+\frac{f}{k_0}k_x,y+\frac{f}{k_0}k_y\right)\exp\left[j\frac{z}{f}(xk_x+yk_y)\right]dxdy \\ &= \mathcal{H}_0\cdot\int_{-\infty}^{+\infty}\int_{-\infty}^{+\infty}\delta\left(\frac{k_0}{f}\left(x+\frac{f}{k_0}k_x\right),\frac{k_0}{f}\left(y+\frac{f}{k_0}k_y\right)\right)\exp\left[j\frac{z}{f}(xk_x+yk_y)\right]dxdy \\ &= \exp\left[-j\frac{z}{2k_0}(k_x^2+k_y^2)\right], \end{aligned}$$

which is the OTF of conventional OSH system. Similarly, the other two terms are

$$
\begin{aligned}
\mathcal{H}_2'(k_x,k_y;z) &= \mathcal{H}_0 \cdot \int_{-\infty}^{+\infty}\int_{-\infty}^{+\infty} t_2'\left(x+\frac{f}{k_0}k_x, y+\frac{f}{k_0}k_y\right)\exp\left[j\frac{z}{f}(xk_x+yk_y)\right]dxdy \\
&= \mathcal{H}_0 \cdot \int_{-\infty}^{+\infty}\int_{-\infty}^{+\infty} \delta\left(\frac{k_0}{f}\left(x+\frac{f}{k_0}k_x\right)-\omega_x, \frac{k_0}{f}\left(y+\frac{f}{k_0}k_y\right)-\omega_y\right)\exp\left[j\frac{z}{f}(xk_x+yk_y)\right]dxdy \\
&= \exp\left[-j\frac{z}{2k_0}(k_x^2+k_y^2)+j\frac{z\omega_x}{k_0}k_x+j\frac{z\omega_y}{k_0}k_y\right] \\
&= \exp\left\{-j\frac{z}{2k_0}\left[(k_x-\omega_x)^2+(k_y-\omega_y)^2\right]\right\} \\
&= \mathcal{H}_1'(k_x-\omega_x, k_y-\omega_y; z),
\end{aligned}
$$

$$
\begin{aligned}
\mathcal{H}_3'(k_x,k_y;z) &= \mathcal{H}_0 \cdot \int_{-\infty}^{+\infty}\int_{-\infty}^{+\infty} t_3'\left(x+\frac{f}{k_0}k_x, y+\frac{f}{k_0}k_y\right)\exp\left[j\frac{z}{f}(xk_x+yk_y)\right]dxdy \\
&= \mathcal{H}_0 \cdot \int_{-\infty}^{+\infty}\int_{-\infty}^{+\infty} \delta\left(\frac{k_0}{f}\left(x+\frac{f}{k_0}k_x\right)+\omega_x, \frac{k_0}{f}\left(y+\frac{f}{k_0}k_y\right)+\omega_y\right)\exp\left[j\frac{z}{f}(xk_x+yk_y)\right]dxdy \\
&= \mathcal{H}_1'(k_x+\omega_x, k_y+\omega_y; z).
\end{aligned}
$$

Therefore we have the OTF of the proposed SI-OSH system

$$
\begin{aligned}
\mathcal{H}'(k_x,k_y;z) &= \mathcal{H}_1'(k_x,k_y;z)+\mathcal{H}_2'(k_x,k_y;z)+\mathcal{H}_3'(k_x,k_y;z) \\
&= \mathcal{H}_1'(k_x,k_y;z)+\mathcal{H}_1'(k_x-\omega_x,k_y-\omega_y;z)+\mathcal{H}_1'(k_x+\omega_x,k_y+\omega_y;z).
\end{aligned} \tag{6}
$$

Note that the first term here represents the original captured hologram in conventional OSH system, while the other two terms refer to the additional information when a patterned illumination is used to project onto the specimen. Compared to the OTF of the conventional OSH system, this one has a larger area in the reciprocal space, meaning that the passband of the low-pass filter is enlarged. That more high frequency components pass through the imaging system leads to the enhancement in spatial resolution. Additionally, an important advantage of the proposed imaging system is that additional images with different phase shifting in the structured illumination microscopy are not necessary in order to extract the high frequency components, which are already contained in the recorded holographic data.[21] The single-short acquisition alleviates the difficulty in mechanical movement of the grating and reduces the recording time. Therefore, the spatial resolution in three dimensions of the OSH imaging system can be improved by introducing a diffraction grating, at the same time without making the acquisition more complicated.

4. RESULTS

According to the principle of SI-OSH, we first simulate the holographic recording and reconstruction of pinhole objects. To verify the improvement of spatial resolution in 2D, we reconstruct one pinhole and two pinholes using OSH and SI-OSH, respectively. The distance between the two pinholes is 10 µm. In the simulation, we let the wavelength of the light source be 532 nm, the focal length of the lens be 20 mm and the radius of the field of view be 0.5 mm, respectively. As such, the NA is 0.025. For the grating, the mean intensity I_0 and modulation depth m are both set to be 1. The period Λ is about 2 µm, which corresponds to 600 grooves per millimeter. The spatial frequency shift, ω_x and ω_y, can be determined using $2\pi/\Lambda$. The reconstruction results as well as the intensity profile across the center are shown in Fig. 4.

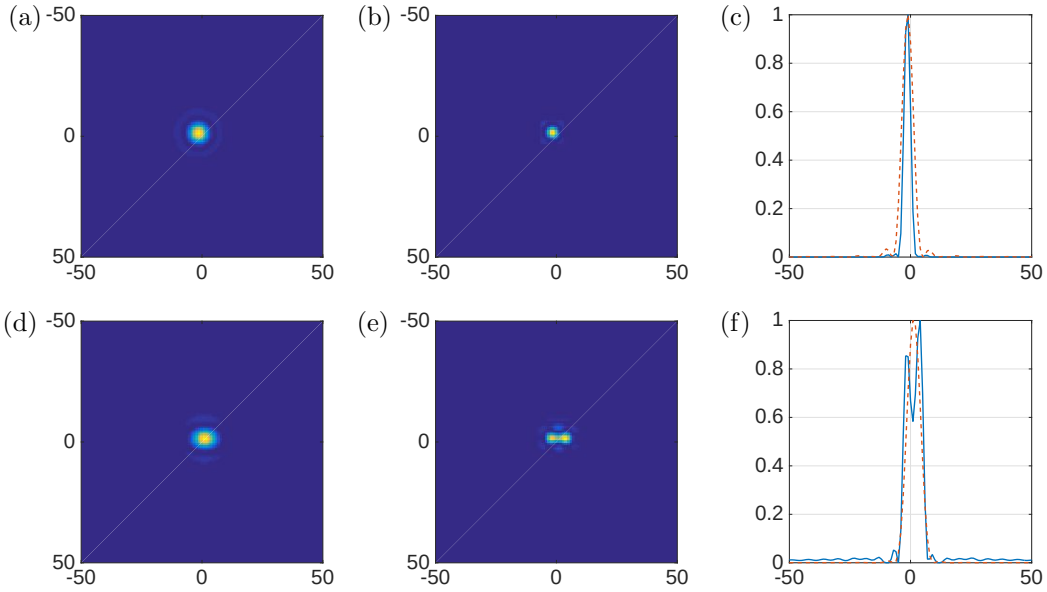

Figure 4: Reconstructions using the conventional OSH and SI-OSH, and intensity profiles along the center in cases of one pinhole ((a), (b) and (c)) and two pinholes ((d), (e) and (f)). Dashed line denotes the conventional OSH. Unit: µm.

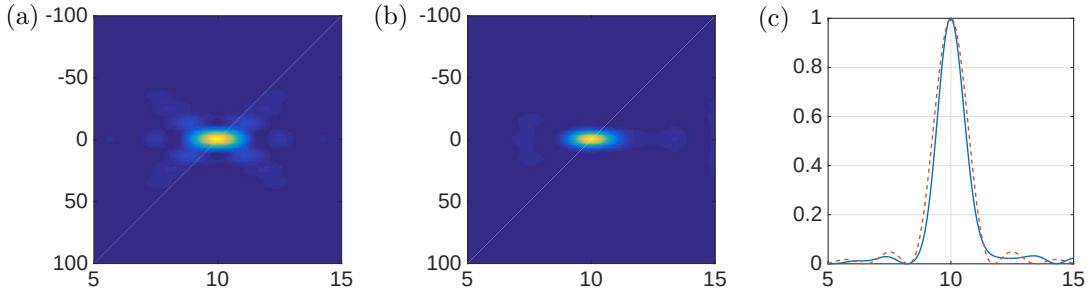

Figure 5: Reconstructions of a pinhole using (a) conventional OSH and SI-OSH (b). (c) Intensity profile across the center of the reconstructed point. Dashed line denotes the conventional OSH. x and y-axis units are mm and µm.

The reconstructions of one pinhole using conventional and proposed OSH systems are presented in Fig. 4(a) and (b). The latter has a narrower intensity profile, as shown in Fig. 4(c). This illustrates the enhancement in lateral resolution. For two pinholes, conventional OSH system cannot distinguish them, as can be seen in Fig. 4(d). However in Fig. 4(e), the two pinholes are clearly discerned. The intensity profile in in Fig. 4(f) also demonstrates the separation.

Theoretically, the diffraction limit of the OSH system in lateral direction is 13.2 µm. The full width at half-maximum (FWHM) values of conventional OSH and SI-OSH are approximately 12.7 µm and 9.5 µm, respectively. The improvement in lateral resolution here is not as high as twofold, which is the extreme capability in scaling down the resolution as shown in Fig. 2. This is due to the fact that the spatial frequency of the grating is below the cutoff frequency of the conventional OTF.

Then we show the resolution enhancement in axial direction. The depth resolution is determined by measuring the defocus size of one pinhole in the reconstruction along the optical axis. Fig. 5(a) and (b) show the images of the conventional OSH and SI-OSH. Similarly, Fig. 5(c) presents the intensity profile across the center line. The theoretical depth resolution is 1.74 mm. The measured FWHM values are approximately 1.62 mm (for

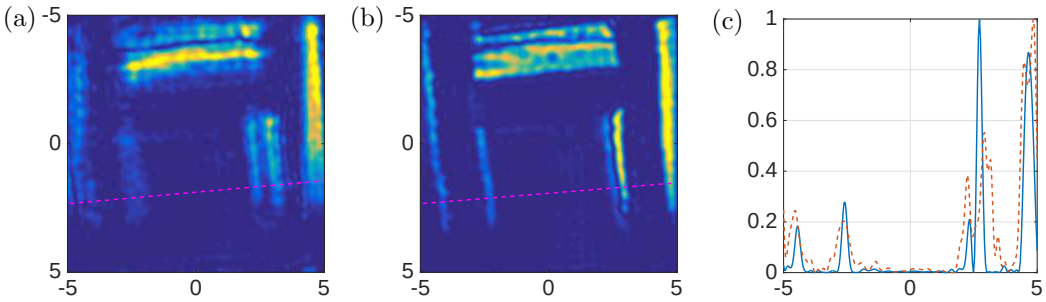

Figure 6: Reconstruction results of experimental data using (a) conventional OSH and (b) SI-OSH. (c) Intensity profile across the center of one point. Dashed line denotes the conventional OSH. x and y-axis units are mm.

conventional OSH) and 1.50 mm (for SI-OSH). In axial direction, the resolution enhancement is minor.

Finally we use experimental data to demonstrate the improvement in lateral resolution. The optical setup is shown in Fig. 3 and the sample is a home-made hollow object "H" (lower part). Reconstruction results are presented in Fig. 6, and Fig. 6(c) presents the intensity profile along a horizontal line. The sharper edges in blue which is recorded by the proposed SI-OSH system denotes the resolution enhancement.

5. CONCLUSIONS

In this paper, we incorporate structured illumination into the OSH imaging system by using a diffraction grating to scale down the spatial resolution beyond the diffraction limit. Compared to structured illumination microscopy, SI-OSH can achieve resolution enhancement using one acquisition. We explain the principle of super-resolution imaging, and verify its feasibility using simulated and experimental data.

ACKNOWLEDGMENTS

This work was supported in part by Research Grants Council of the Hong Kong Special Administrative Region, China, under NSFC/RGC Project N_HKU714/13.

REFERENCES

[1] Kim, M. K., "Principles and techniques of digital holographic microscopy," *SPIE Reviews* **1**(1), 018005 (2010).

[2] Marquet, P., Rappaz, B., Magistretti, P. J., Cuche, E., Emery, Y., Colomb, T., and Depeursinge, C., "Digital holographic microscopy: a noninvasive contrast imaging technique allowing quantitative visualization of living cells with subwavelength axial accuracy," *Optics Letters* **30**(5), 468–470 (2005).

[3] Yamanaka, M., Smith, N. I., and Fujita, K., "Introduction to super-resolution microscopy," *Microscopy* **63**(3), 177–192 (2014).

[4] Liu, C., Liu, Z., Bo, F., Wang, Y., and Zhu, J., "Super-resolution digital holographic imaging method," *Applied Physics Letters* **81**(17), 3143–3145 (2002).

[5] Indebetouw, G., Tada, Y., Rosen, J., and Brooker, G., "Scanning holographic microscopy with resolution exceeding the rayleigh limit of the objective by superposition of off-axis holograms," *Applied Optics* **46**(6), 993–1000 (2007).

[6] Ke, J., Poon, T.-C., and Lam, E. Y., "Depth resolution enhancement in optical scanning holography with a dual-wavelength laser source," *Applied Optics* **50**(34), H285–H296 (2011).

[7] Ou, H., Poon, T.-C., Wong, K. K., and Lam, E. Y., "Depth resolution enhancement in double-detection optical scanning holography," *Applied Optics* **52**(13), 3079–3087 (2013).

[8] Lam, E. Y., Zhang, X., Vo, H., Poon, T.-C., and Indebetouw, G., "Three-dimensional microscopy and sectional image reconstruction using optical scanning holography," *Applied Optics* **48**(34), H113–H119 (2009).

[9] Chan, A. C., Tsia, K. K., and Lam, E. Y., "Subsampled scanning holographic imaging (SuSHI) for fast, non-adaptive recording of three-dimensional objects," *Optica* **3**(8), 911–917 (2016).
[10] Poon, T.-C., [*Optical Scanning Holography with MATLAB*], Springer-Verlag, New York, first ed. (2007).
[11] Chen, N., Ren, Z., Ou, H., and Lam, E. Y., "Resolution enhancement of optical scanning holography with a spiral modulated point spread function," *Photonics Research* **4**(1), 1–6 (2016).
[12] Poon, T.-C., "Scanning holography and two-dimensional image processing by acousto-optic two-pupil synthesis," *Journal of the Optical Society of America A* **2**(4), 521–527 (1985).
[13] Ou, H., Poon, T.-C., Wong, K. K., and Lam, E. Y., "Enhanced depth resolution in optical scanning holography using a configurable pupil," *Photonics Research* **2**(2), 64–70 (2014).
[14] Zhang, X., Lam, E. Y., and Poon, T.-C., "Reconstruction of sectional images in holography using inverse imaging," *Optics Express* **16**, 17215–17226 (2008).
[15] Gustafsson, M. G., "Surpassing the lateral resolution limit by a factor of two using structured illumination microscopy," *Journal of Microscopy* **198**(2), 82–87 (2000).
[16] Gustafsson, M. G., "Nonlinear structured-illumination microscopy: wide-field fluorescence imaging with theoretically unlimited resolution," *Proceedings of the National Academy of Sciences of the United States of America* **102**(37), 13081–13086 (2005).
[17] Gustafsson, M. G., Shao, L., Carlton, P. M., Wang, C. R., Golubovskaya, I. N., Cande, W. Z., Agard, D. A., and Sedat, J. W., "Three-dimensional resolution doubling in wide-field fluorescence microscopy by structured illumination," *Biophysical Journal* **94**(12), 4957–4970 (2008).
[18] Saxena, M., Eluru, G., and Gorthi, S. S., "Structured illumination microscopy," *Advances in Optics and Photonics* **7**(2), 241–275 (2015).
[19] Ma, J., Yuan, C., Situ, G., Pedrini, G., and Osten, W., "Resolution enhancement in digital holographic microscopy with structured illumination," *Chinese Optics Letters* **11**(9), 090901 (2013).
[20] Gao, P., Pedrini, G., and Osten, W., "Structured illumination for resolution enhancement and autofocusing in digital holographic microscopy," *Optics Letters* **38**(8), 1328–1330 (2013).
[21] Ströhl, F. and Kaminski, C. F., "Frontiers in structured illumination microscopy," *Optica* **3**(6), 667–677 (2016).